



Cite this: *Chem. Commun.*, 2019, 55, 10654

## Cucurbit[*n*]uril-based amphiphiles that self-assemble into functional nanomaterials for therapeutics

Kyeng Min Park,<sup>id</sup>\*<sup>a</sup> Moon Young Hur,<sup>a</sup> Suman Kr Ghosh,<sup>a</sup> Deepak Ramdas Boraste,<sup>a</sup> Sungwan Kim<sup>b</sup> and Kimoon Kim<sup>id</sup>\*<sup>ab</sup>

Some host–guest complexes of cucurbit[*n*]uril (CB[*n*]) host molecules act as supramolecular amphiphiles (SAs), which hierarchically self-assemble into various nanomaterials such as vesicles, micelles, nanorods, and nanosheets in water. The structures and functions of the nanomaterials can be controlled by supramolecular engineering of the host–guest complexes. In addition, functionalization at the periphery of CB[6] and CB[7] generates CB[*n*]-based molecular amphiphiles (MAs) that can also self-assemble into vesicles or micelle-like nanoparticles in water. Taking advantage of the molecular cavities of CBs and their strong guest recognition properties, the surface of the self-assembled nanomaterials can be easily decorated with various functional tags in a non-covalent manner. In this feature article, the two types (SAs and MAs) of CB-based amphiphiles, their self-assemblies and their applications for nanotherapeutics and theranostics are presented with future perspectives.

Received 18th July 2019,  
Accepted 8th August 2019

DOI: 10.1039/c9cc05567c

rsc.li/chemcomm

### Introduction

Amphiphiles are molecules typically possessing both hydrophilic and lipophilic moieties, such as polar heads and long alkyl tails, as exemplified by phospholipids in nature. Amphiphiles in water

tend to maximize contact between their hydrophilic moieties and water molecules, while minimizing exposure of the lipophilic moieties to water and optimizing interactions among molecules.<sup>1</sup> Thus, they eventually self-assemble into stabilized nanostructures in aqueous solutions, such as membranes, vesicles, micelles, tubes, and wires, depending on their molecular structures.<sup>2</sup> Rational design of molecular and polymeric amphiphiles with well-balanced hydrophilic and lipophilic moieties has facilitated the development of various nanomaterials with different chemical and physical functions.<sup>3,4</sup> Typically, hydrophilic and

<sup>a</sup> Center for Self-Assembly and Complexity, Institute for Basic Science (IBS), Pohang, 37673, Republic of Korea. E-mail: kmpark@ibs.re.kr; Web: <http://csc.ibs.re.kr>

<sup>b</sup> Department of Chemistry, Pohang University of Science and Technology, Pohang, 37673, Republic of Korea. E-mail: kkim@postech.ac.kr



**Kyeng Min Park**

*Kyeng Min Park studied supramolecular chemistry at POSTECH (PhD 2009) in Korea. After 2 years postdoctoral research in chemistry and chemical biology at Harvard University, he returned to Korea to work for Samsung Electronics as a senior researcher until 2014. Then, he joined to the Institute for Basic Science (IBS) where he is now a group leader in the Center for Self-assembly & Complexity (CSC) and focusing on developing supramolecular materials and tools for chemical biology and theranostics.*



**Moon Young Hur**

*Moon Young Hur received his PhD degree in organic chemistry from the University of Kansas (U. S. A.) in 2015. After 2 years postdoctoral work at the Institute for Basic Science (IBS) and 1 year at Korea Research Institute of Chemical Technology (KRICT), he returned to IBS where he is now a Research Fellow at CSC. His current research focuses on the development of novel synthetic methods for the preparation of cucurbiturils and derivatives, and their applications for self-assembled materials for chemical biology.*

lipophilic units are conjugated to each other through covalent linkages to afford an amphiphile, which often results in low yield *via* a multistep synthetic process. Furthermore, additional synthesis is required not only for tuning the amphiphilicity of molecules, but also for conferring functions on amphiphiles, such as stimuli-responsiveness. Supramolecular chemistry provides a new approach for developing new types of functional amphiphiles, especially supramolecular amphiphiles (SA) composed of molecular assemblies *via* non-covalent interactions including hydrogen bonds,  $\pi$ - $\pi$  interactions, electrostatic interactions, charge transfer interactions, and host-guest interactions.<sup>5-7</sup> Among them, host-guest interactions have been exploited as a useful functional motif for designing SAs since interactions between hosts and guests are reversible, controllable, and responsive to environmental changes.<sup>6</sup> Among well-known host molecules that form complexes with guests, cucurbit[*n*]urils (CB[*n*], *n* = 5-8, 10, 13-15)<sup>8,9</sup> have great potential as SAs, since CB[*n*]s form exceptionally strong and stable host-guest complexes in water, which is beneficial to designing reliable supramolecular assemblies.<sup>10-14</sup>

Such unique host-guest interactions are mostly attributed to the rigid molecular structure of CB[*n*]s, consisting of hydrophobic cavities and two identical and symmetric carbonyl-laced portals. Selected guests with positive charges can fit snugly into the hydrophobic inner cavity *via* complementary charge-dipole interactions with the carbonyl portals of CB[*n*]s, forming strong and stable host-guest complexes with CB[*n*]s in water. For example, CB[6] forms a stable 1 : 1 host-guest complex with alkylammonium compounds such as spermine (spm) and spermidine (spmd) with high binding affinity ( $K_a = \sim 10^{11}$ - $10^{12}$  M<sup>-1</sup> in water).<sup>15</sup> Similarly, CB[7] efficiently accommodates ferrocenemethyl- (FcA) and adamantyl-ammonium (AdA) in its cavity with remarkably high binding affinity ( $K_a = \sim 10^{12}$ - $10^{15}$  M<sup>-1</sup> in water).<sup>16-22</sup> Interestingly, CB[8] can accommodate a pair of molecules such as methyl viologen (MV) and 2,6-dihydroxynaphthalene (DHNp) in its cavity to form a stable 1 : 1 : 1 ternary host-guest complex. The interaction among the three components ( $K_a = \sim 10^{11}$  M<sup>-2</sup> in 10 mM sodium phosphate buffer)<sup>23,24</sup> is sufficiently strong to hold them together, thereby promoting self-assembly of the ternary complex into



**Suman Kr Ghosh**

*Suman Kr Ghosh received both his BSc (2009) and MSc (2011) degrees in chemistry from the University of Calcutta, India. He then obtained his PhD (2017) from the University of Hyderabad, working with Prof. R. Nagarajan on synthesis of heterocycles. Currently, he is working as a postdoctoral research fellow at CSC, IBS.*



**Deepak Ramdas Boraste**

*Deepak Ramdas Boraste received both his BSc (2003) and MSc (2005) degrees in chemistry from the University of Pune, India. He has worked as a research and development scientist at Acoris Research Limited, Pune, India. He then obtained his PhD (2019) from the Institute of Chemical Technology, Mumbai, at the Department of Dyestuff Technology working on the "Synthesis and applications of supramolecular host: Cucurbit[7]uril". Currently, he is working as a postdoctoral research fellow at CSC, IBS.*



**Sungwan Kim**

*Sungwan Kim received his BSc (2014) degree in chemistry from the Pusan National University, Korea. Then, he joined the laboratory of Prof. Kimoon Kim at POSTECH in 2014 to pursue his PhD in chemistry. His current research interest is supramolecular chemistry for biomedical applications.*



**Kimoon Kim**

*Kimoon Kim studied chemistry at Seoul National University (BS, 1976), Korea Advanced Institute of Science and Technology (MS, 1978), and Stanford University (PhD, 1986). After two-years of postdoctoral work at Northwestern University, he joined POSTECH where he is now Distinguished University Professor. Since 2012, he has also been the director of Center for Self-assembly and Complexity (CSC), Institute for Basic Science (IBS). His current research focuses on developing novel functional materials and systems based on supramolecular chemistry.*





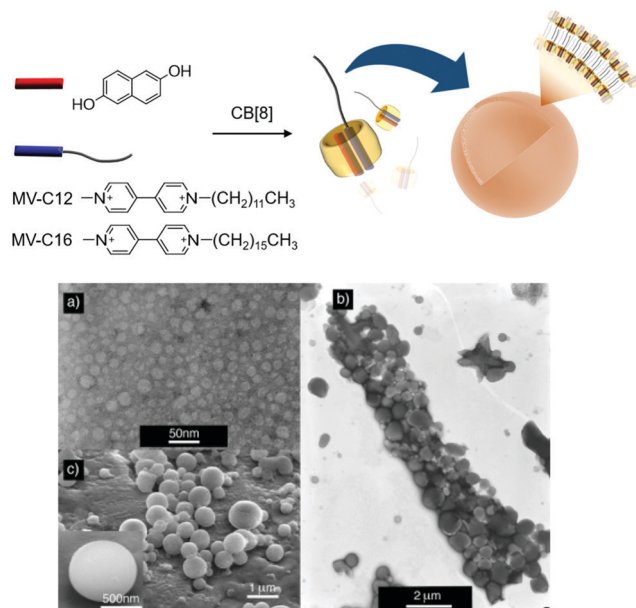


**Fig. 2** Formation of vesicles with a ternary complex of MV-C12 (or MV-C16), DHNp, and CB[8] as a SA. (a) TEM image of vesicles formed by MV-C12, DHNp, and CB[8]. (b) TEM and (c) SEM images of vesicles formed by MV-C16, DHNp, and CB[8]. TEM and SEM images adapted from ref. 25 with permission from Wiley-VCH.

scanning electron microscopies (TEM and SEM) revealed that small vesicles with an average diameter of 20 nm are formed by a ternary complex made of CB[8] with DHNp and MV-C12 (Fig. 2a), whereas larger complexes with a diameter ranging from 400 to 950 nm are formed by another ternary complex with MV-C16 instead of MV-C12 (Fig. 2b and c). It seems that a longer alkyl tail in the SA induces a larger membrane curvature, resulting in larger vesicles. These results and the associated analysis suggest that vesicles can be formed as hierarchical self-assemblies with SAs through CB[8]-based host-guest interactions, and their size can be controlled by a simple alteration of the guest of CB[8].

Scherman and colleagues subsequently reported vesicles made from another CB[8]-based ternary complex that act as a guest-responsive cytotoxic nanomaterial.<sup>38</sup> In this study, an amphiphilic ternary complex was formed by the inclusion of a CT complex between pyrenylimidazolium-conjugated hexameric peptide (PyIm-GGGKKK) and MV-conjugated C18 (MV-C18) inside CB[8]. This SA eventually self-assembles into vesicles with an average diameter of 200 nm, as confirmed by TEM and dynamic light scattering (Fig. 3). The PyIm unit in PyIm-GGGKKK serves as a fluorescent probe that can indicate the assembly and disassembly of the CT complex by quenching and dequenching of the fluorescence signal, respectively. The guest can be exchanged due to the dynamic nature of the host-guest interactions. Treatment with DHNp as an electron donor guest that competes with the PyIm moiety leads to the release of PyIm-GGGKKK into the culture media through the formation of a different ternary complex with DHNp and MV-C18 in CB[8]. This guest exchange induces the rupture of vesicles, converting them into insoluble particles due to significantly reduced amphiphilicity of the ternary complex. The release of the

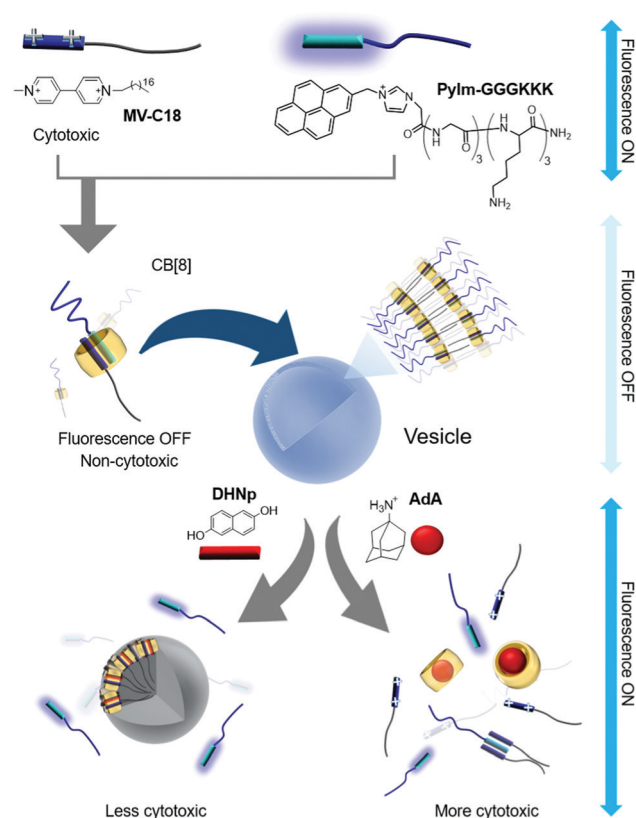


**Fig. 3** Self-assembly of a ternary complex of MV-C18, PyIm-GGGKKK, and CB[8] as a SA into vesicles, and disruption of vesicles upon treatment with competitive guests.

hydrophilic PyIm-GGGKKK from the ternary complex into the media is immediately detected by the simultaneous appearance of fluorescence from the PyIm moiety. When treated with AdA, a larger guest than DHNp, vesicles also collapse since AdA occupies the cavity of CB[8] alone and releases both the guests (MV-C18 and PyIm-GGGKKK) from CB[8], resulting in the enhancement of the fluorescence signal from the released PyIm-GGGKKK. Overall, the release of guests from the ternary complex followed by the collapse of vesicles can be controlled by a dynamic guest exchange and visualized by fluorescent signal changes. Fluorescent nanomaterials with structural controllability on demand are useful for the delivery of drugs into cells. Cell experiments were performed using these vesicles, and their disruption was observed inside the cells using a confocal laser scanning microscope following treatment with competitive guests (DHNp and AdA) by visualizing the fluorescent signal accompanying the release of PyIm-GGGKKK from the ternary complex. Cytotoxicity assays revealed that these vesicles are more cytotoxic when treated with AdA than with DHNp, probably due to a greater release of cytotoxic MV-C18 into the media. This study demonstrated that utilization of a CB[8]-based SA formed *via* well-designed, sensitive, and dynamic host-guest interactions can yield novel nanotherapeutic systems that not only release drugs on demand upon treatment with competitive guests, but also exhibit altered fluorescent signals that facilitate visualization of drug release inside living cells. The use of the ternary complex with a pair of PyIm and MV inside

CB[8] was later extended to the formation of thermo-responsive vesicles by conjugation of a temperature-sensitive poly-*N*-isopropylacrylamide (PNIPAAm) to MV, forming a CT complex with PyIm-GGGKKK inside CB[8].<sup>39</sup> Upon increasing the temperature to 37 °C, the ternary complex self-assembles into vesicles *via* enhanced hydrophobicity of the PNIPAAm moiety acting as a hydrophobic tail in the SA. These vesicles formed at 37 °C are coated with GGGKKK peptides, which is beneficial for entrapping temperature-sensitive proteins such as basic fibroblast growth factor (bFGF).

In the following year, Jin and Ji developed another CB[8]-based ternary complex that acts as a supramolecular block-copolymer amphiphile to spontaneously form micelle-like nanoaggregates.<sup>41</sup> In this study, indole and MV derivatives were used as an electron donor and acceptor, respectively, to form a CT complex inside CB[8]. Amphiphilicity in the ternary complex was achieved by exploiting hydrophilic and lipophilic linear polymers such as poly-lactic acid (PLA) and polyethyleneglycol (PEG) conjugated to indole (ID-PLA) and MV (MV-PEG), respectively (Fig. 4a). Although the structure of the supramolecular assembly in the micelle-like nanoparticles is yet to be clearly characterized, the core of the particle is hydrophobic enough to efficiently entrap a drug such as doxorubicin (DOX) inside. Reduction-responsive dissociation of the CT complex triggers transformation of the micelles into larger particles up to 1 μm in diameter upon treatment with a reducing agent such as sodium dithionite (Na<sub>2</sub>S<sub>2</sub>O<sub>4</sub>), mostly due to aggregation of hydrophobic PLA dissociated from the SA under reducing conditions. This redox-responsive behavior of host-guest interactions facilitates the reduction-responsive release of DOX loaded inside the particles. In a later study, pH-responsive release of DOX was also demonstrated with another micelle-like nanoaggregate ~150 nm in size formed by the ternary complex of a CT pair,<sup>40</sup> naphthalene conjugated to PEG (Np-PEG), and MV linked to DOX through an acid-labile hydrazone bond (MV-DOX, a prodrug) inside CB[8] (Fig. 4b). After the particles are internalized into cells, the prodrug localized inside the self-assembled particles is released

as a drug (DOX) in acidic organelles (lysosomes; pH ~ 5.0–5.5), where the hydrazone moiety is cleaved. A conceptually similar work was reported by Tang, Chen and colleagues.<sup>42</sup> They used a brush copolymer having tetraphenyl ethane (TPE) and MV moieties as guests forming a ternary complex with PEG-conjugated naphthalene inside the CB[8] cavity. This CB[8]-based ternary complex also acts as a SA forming micelle-like nanoparticles. The fluorescence signal of TPE was quenched upon loading DOX inside the nanoparticles; the disassembly of SNPs through intracellular reducing agents and low pH environment allowed visualization of the drug release inside cancer cells. Moreover, the authors provided *in vivo* results showing enhanced drug efficacy to cancer-bearing mice with their DOX-loaded nanoparticles compared to free DOX, demonstrating the potential of the CB[8]-based nanomaterial as a promising nanotherapeutic technology. Recently, Huang, Luo and colleagues reported a light responsive ternary complex as a SA formed by two guests inside CB[8]; a MV derivative and a *trans*-azobenzene derivative conjugated to a tris(*n*-dodecyloxy)benzyl unit.<sup>43</sup> The SA was found to form vesicles entrapping DOX. UV light induced *trans* to *cis* isomerization of the azo moiety facilitates dissociation of the guest from the host-guest complex; thus the DOX-loaded vesicles were eventually ruptured to release DOX inside cancer cells.

CB[8]-based ternary complexes as SAs can be systematically designed to tune the morphology, size, and function of self-assembled nanomaterials by altering hydrophilic and lipophilic moiety-conjugated guests using host-guest chemistry as discussed above. In addition, the stimuli-responsiveness and negligible toxicity of CB[8]<sup>44</sup> offer great potential for CB[8]-based SAs as novel building blocks to provide functional nanomaterials for storage of sensitive biomolecules such as proteins, and efficient entrapment and controlled release of hydrophobic drugs.

Host-guest complexes between guests and CB[7] can also act as SAs that spontaneously organize to form nanomaterials in water. Recently, Nau and colleagues reported a SA consisting of a 1:1 host-guest complex between pyridinium-conjugated anthracene (AnPy) and CB[7], which forms solid nanoparticles

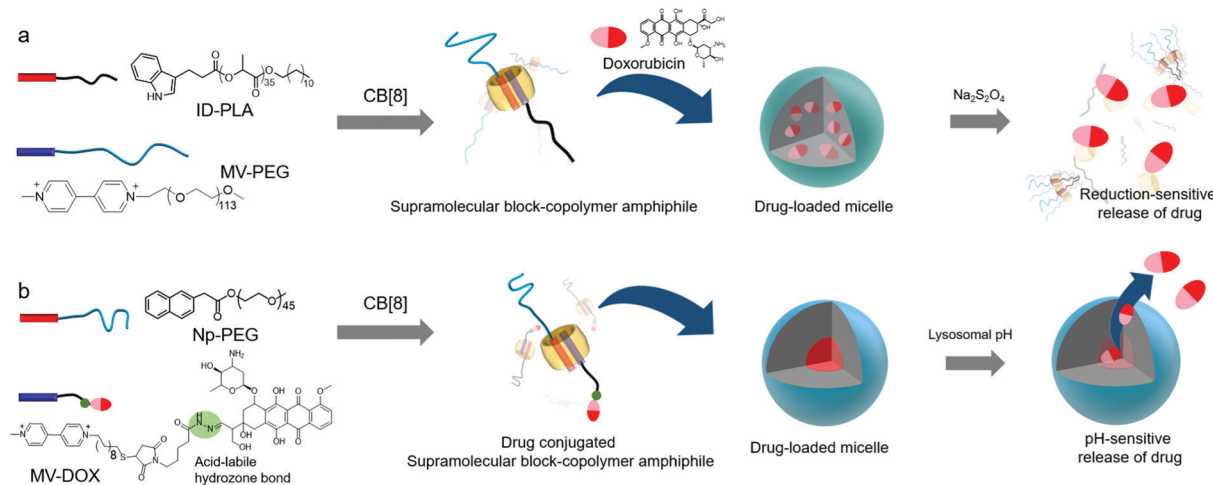


Fig. 4 Schematic illustration of the formation of micelles with CB[8]-based SAs. (a) Reduction- and (b) pH-sensitive drug release.

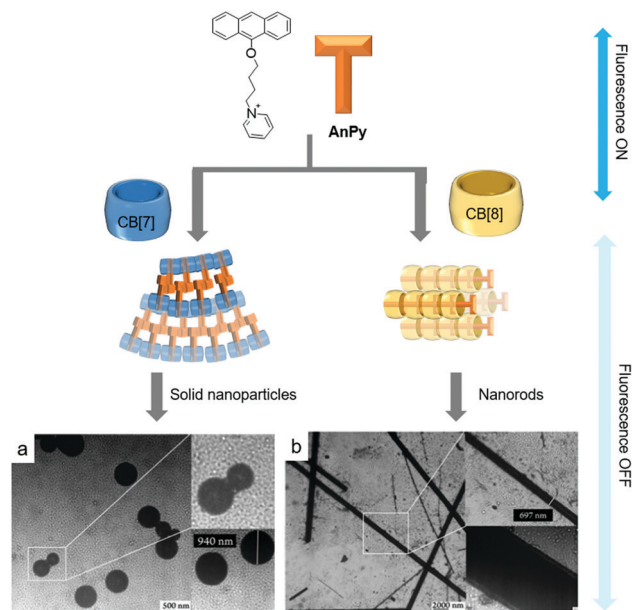


Fig. 5 Proposed molecular assemblies of SAs formed by (a) AnPy@CB[7] and (b) AnPy@CB[8], with their TEM images. TEM images are reproduced from ref. 43 with permission from The Royal Society of Chemistry.

with diameters ranging from 400 to 1000 nm in water (Fig. 5a).<sup>45</sup> When AnPy interacts with CB[7] (AnPy@CB[7],  $K_a \sim 10^4 \text{ M}^{-1}$ ), the pyridinium moiety is included in CB[7] while the anthracenyl unit is located outside CB[7]. The authors reported that anthracenyl units from different AnPy molecules interact with each other *via*  $\pi$ - $\pi$  stacking, which is believed to be critical for the formation of nanoparticles with AnPy@CB[7]. Unlike AnPy@CB[7], AnPy interacts with CB[8] (AnPy@CB[8],  $K_a \sim 10^6 \text{ M}^{-1}$ ) in water to self-assemble into nanorods up to a few micrometers in length and  $\sim 700 \text{ nm}$  in width. Since CB[8] has a larger cavity than CB[7], it can accommodate both anthracenyl and pyridinium units in the cavity; hence it was proposed that complexation of pyridinium and anthracene residues from different molecules inside CB[8] facilitates the formation of supramolecular polymeric chains that interact with each other through the outer surface of CB[8] to form nanorods (Fig. 5b). This study demonstrated that different self-assembled nanostructures can be prepared by simple mixing of an appropriate host molecule with a guest.

In 2013, Zhang and colleagues developed a non-linear SA formed from a tetranaphthalenylmethylpyridinium-conjugated porphyrin (TPOR) and CB[7].<sup>46</sup> Each naphthalenyl moiety on TPOR is included in the cavity of CB[7] ( $K_a \sim 10^7 \text{ M}^{-1}$ ); hence four CB[7]s come together to form a complex with a single TPOR molecule (CB[7]<sub>4</sub>/TPOR; Fig. 6). TPOR possesses four positive charges on its pyridinium and acts as an amphiphile itself, forming nanoparticles in water (Fig. 6a) with significant fluorescence quenching due to close stacking between TPOR molecules. Furthermore, CB[7]<sub>4</sub>/TPOR complexes act as SAs and self-assemble into nanosheets (Fig. 6b) that emit strong fluorescence, unlike nanoparticles formed by TPOR alone. In this case, CB[7]-based host-guest chemistry plays an important

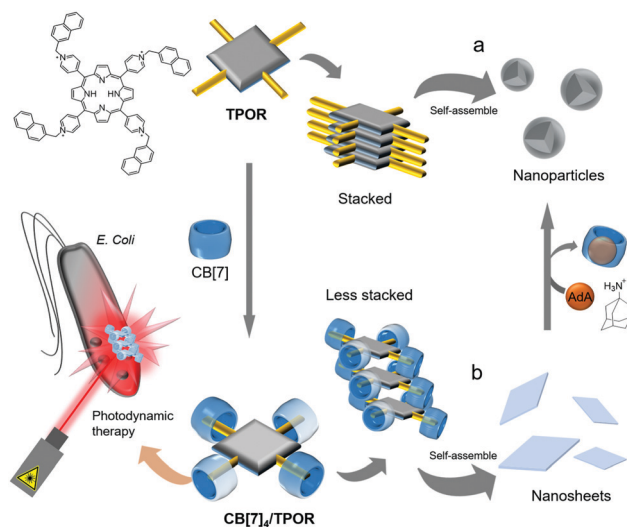


Fig. 6 Self-assemblies of (a) TPOR and (b) CB[7]<sub>4</sub>/TPOR and their applications as photosensitizers for photodynamic therapy.

role not only in altering the self-assembled structure of TPOR from nanoparticles to nanosheets, but also in suppressing the stacking of TPOR by introducing bulky units such as CB[7].

Porphyrins have been widely used as photosensitizers to generate highly reactive singlet oxygen upon light irradiation, causing cytotoxicity and severe damage to cellular components. However, porphyrins typically suffer from unwanted stacking between molecules, which significantly reduces the efficiency of singlet oxygen generation in photodynamic therapy. CB[7]<sub>4</sub>/TPOR-based nanosheets with TPOR suffer less from unwanted stacking and serve as an efficient photosensitizer to kill Gram-negative *Escherichia coli* bacteria more efficiently than nanoparticles formed by closely stacked TPOR, suggesting that CB[7]-based SAs are superior for photocytotoxicity. In addition, when treated with AdA, CB[7] is released from CB[7]<sub>4</sub>/TPOR to form a host-guest complex with AdA that has a much stronger binding affinity to CB[7] ( $K_a \sim 10^{12} \text{ M}^{-1}$ ) than the naphthalenyl unit, resulting in the conversion of nanosheets back to nanoparticles, and consequent quenching of fluorescence emission. The guest-responsive transformation of nanostructures and changes in optical properties suggest that this SA formed by host-guest interactions between a porphyrin derivative and CB[7] can be exploited as a smart functional nanomaterial. Furthermore, in addition to antibacterial action, this system can be utilized for anticancer treatment.

In a later study, Isaacs and colleagues carefully designed a conjugate of CB[6] to CB[7] (CB[6-7]), and used it as a double-cavity host molecule to generate SAs formed from a host-guest complex with 1,6-diammoniumhexane-conjugated C18 alkyl chain (DAH-C18) and 1-adamantanemethylammonium-conjugated PEG5000 (AdMA-PEG; Fig. 7).<sup>29</sup> Since CB[6-7] has two different cavities in each molecule, it can accommodate the same or different guests to form homodimer or heterodimer complexes, respectively. The linear DAH moiety can be included in both cavities, and CB[6-7] forms a homodimer complex with two



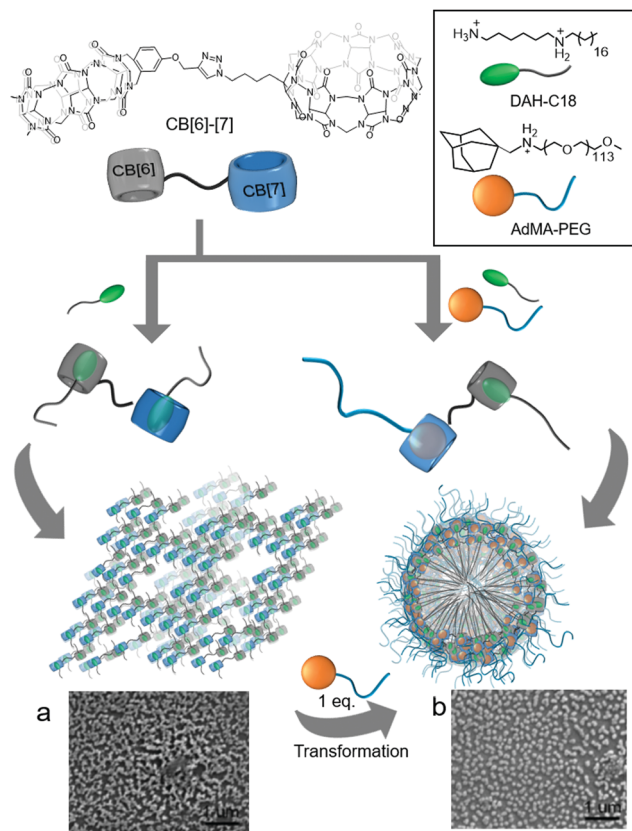


Fig. 7 Proposed supramolecular assemblies of host-guest complexes of CB[6]-[7] with (a) DAH-C18 (a homodimer form) and (b) DAH-C18 and AdA-PEG (a heterodimer form), with their SEM images. SEM images are reproduced from ref. 29 with permission from The Royal Society of Chemistry.

DAH-C18 molecules ( $\text{DAH-C18}_2@CB[6-7]$ ) and spontaneously self-assembles into a connected network structure through hydrophobic interactions between the long alkyl chains (Fig. 7a). The AdMA moiety is larger than DAH and cannot form a complex with CB[6], but it fits well inside the CB[7] cavity. When DAH-C18 and AdMA-PEG are added at a 1:1 ratio, a heterodimer complex ( $[\text{DAH-C18} + \text{AdMA-PEG}]@CB[6-7]$ ) is formed with 1 eq. of CB[6-7] as a SA, and this hierarchically self-assembles into micelle-like particles with an average diameter of 125 nm (Fig. 7b). Furthermore, hydrophobic interactions induced by the C18 unit in the SA play a crucial role in forming a hydrophobic core with hydrophilic PEG moieties exposed to water on the surface of the molecule. Since CB[7] has higher binding affinity to AdMA ( $K_a \sim 10^{14} \text{ M}^{-1}$ ) than to DAH ( $K_a \sim 10^7 \text{ M}^{-1}$ ), treatment of the  $\text{DAH-C18}_2@CB[6-7]$  network with AdMA-PEG (1 eq.) induces the exchange of DAH-C18 bound in the cavity of CB[7], causing self-sorting of AdMA-PEG that converts  $\text{DAH-C18}_2@CB[6-7]$  into  $[\text{DAH-C18} + \text{AdMA-PEG}]@CB[6-7]$ , resulting in morphological transformation to nanoparticles. This work demonstrated the ability of a double-cavity host molecule to control the morphology of nanostructures using guest-specific formation of dynamic SAs based on a supramolecular self-sorting concept.

## CB[n]-based molecular amphiphiles (MAs)

Functionalization of CB[n] allows fine-tuning of the solubility of CB[n] derivatives. For example, CB[6] is not soluble and precipitates in water. However, conjugation of hydrophilic groups to CB[6] enables CB[6] derivatives to act as MAs that form self-assembled nanomaterials such as vesicles<sup>32,34</sup> and micelle-like nanoparticles<sup>33</sup> with good dispersibility in water. Interestingly, functionalization takes place at the periphery of CB[n] to generate unconventional amphiphiles with flexible functional arms at the periphery of a rigid CB[n]. The molecular structures of amphiphilic CB[n] derivatives are different from those of conventional amphiphiles possessing two different well-defined units such as a polar head and a long lipophilic tail. Given the structural features of amphiphilic CB[n] derivatives, interesting and useful self-assembled functional nanomaterials can be prepared. In this section, various amphiphilic CB[n] derivatives, their self-assemblies, and their bioapplications are discussed.

In 2005, we reported the synthesis of the first amphiphilic CB[n] derivative, namely, a tetraethylglycol (TEG)-tethered CB[6] derivative (TEG-CB[6]) formed *via* a thiol-ene photoreaction between thiolated TEG and perallyloxyated CB[6] (Fig. 8a).<sup>32</sup> It is not possible to define hydrophilic and hydrophobic moieties in TEG-CB[6]. However, TEG-CB[6] was revealed to be an amphiphile in water that self-assembles into enclosed membrane structures such as vesicles (CB[6]VCs) with average diameter ranging from 30 to 1000 nm and a shell thickness of 6 nm (Fig. 8). After extrusion of CB[6]VCs through a membrane with 200 nm pores, the average diameter of the vesicles was changed to 170 nm with the same membrane thickness due to the dynamic nature of a self-assembled membrane (Fig. 8c). The packing structure of TEG-CB[6] in the shell is not yet clearly understood. Given that the hollow structure of CB[6]VCs is not disrupted even after treatment with a strong surfactant such as Triton X-100, the packing structure of TEG-CB[6] is likely to be sufficiently robust to avoid interference from conventional surfactants. In addition, the membrane of CB[6]VCs includes a number of cavities of CB[6]s that form a strong and stable host-guest complex with linear polyammonium compounds such as spm and spmd with a high binding affinity ( $K_a \sim 10^{11}-10^{12} \text{ M}^{-1}$ ). Thus, a large number of functional tags conjugated to spm or spmd can be introduced onto the surface of CB[6]VCs easily in a non-covalent manner, as confirmed by confocal laser scanning microscopy analysis of CB[6]VCs coated with fluorescein isothiocyanate-conjugated spm (FITC-spm@CB[6]VCs; Fig. 8d). CB[6]VCs with a robust membrane made from a large number of TEG-CB[6] can be utilized as a multivalent scaffold for enhanced molecular recognition of a binding ligand to its target protein, such as sugars to lectins. For example, the binding constant of  $\alpha$ -mannose-conjugated spmd-coated CB[6]VCs (Man-spm@CB[6]VCs) to Concanavalin A (ConA, a lectin for  $\alpha$ -mannose recognition) was three orders of magnitude stronger than that of Man-spm, as quantified by surface plasmon resonance experiments, clearly demonstrating that CB[6]VCs can serve as a novel multivalent scaffold for enhanced

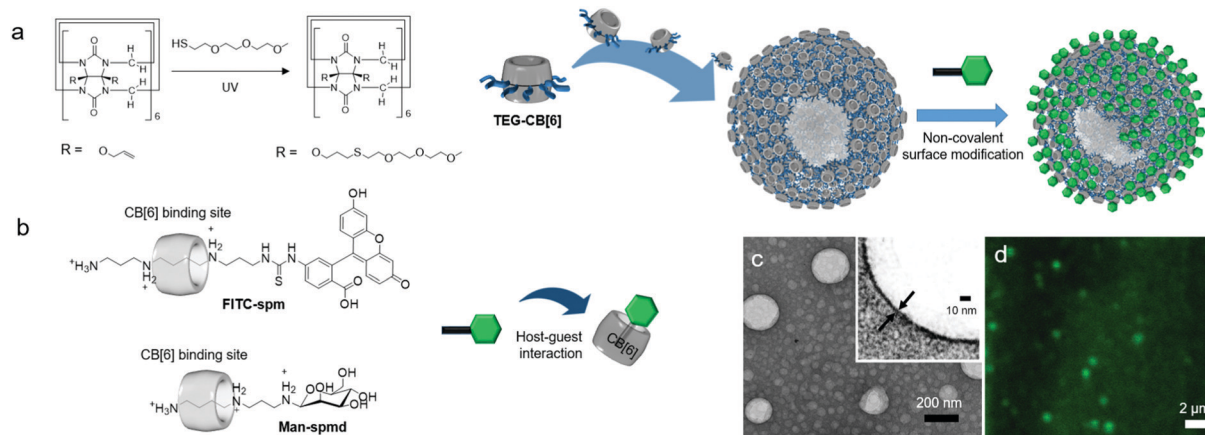


**Fig. 8** Formation of CB[6]VCs, and their non-covalent surface modification. (a) Synthetic scheme of TEG-CB[6]. (b) Chemical structures of FITC-spm and Man-spm. (c) TEM image of CB[6]VCs. (d) Confocal laser scanning microscopy image of FITC-spm@CB[6]VCs. TEM and confocal laser scanning microscopy images are reproduced from ref. 32 with permission from American Chemical Society.

molecular recognition. Furthermore, various different functional tags can be introduced onto the scaffold through simple mixing of different functional spmd-linked tags to afford multifunctional nanomaterials.

Following this, we developed reduction-sensitive amphiphilic CB[6] derivatives (HEG-SS-CB[6]) by insertion of a disulfide bond between CB[6] and hexaethyleneglycol (HEG) arms. HEG-SS-CB[6] also acts as a MA in water, spontaneously forming vesicles (SSCB[6]VCs; Fig. 9). Repeated extrusion of SSCB[6]VCs through a membrane with 200 nm pores generates uniform vesicles of 170 nm in diameter and a membrane thickness of 6 nm (Fig. 9c), very similar in size and morphology to CB[6]VCs formed by TEG-CB[6] without disulfide linkages.<sup>34</sup>

Leakage of drugs loaded within typical lipid-based vesicles before reaching a target site can cause unwanted side effects, potentially killing normal healthy cells. The robust membrane of SSCB[6]VCs does not collapse under physiological conditions; hence the inner space entrapping drugs remains intact, and the reduction-responsiveness of the MA allows cleavage inside cells, and easy surface modification with a functional tag conjugated to spm (or spmd), as demonstrated for folate-conjugated

spm (folate-spm). Thus, SSCB[6]VCs can serve as a reduction-sensitive cancer-targeted drug delivery vehicle. This was confirmed experimentally by confocal laser scanning microscopy of live cells under various conditions with vesicles such as folate-spm@SSCB[6]VCs loaded with DOX, as well as SSCB[6]VCs without folate-spm or folate-spm@CB[6]VCs. HeLa cells treated with SSCB[6]VCs did not display a significant fluorescent signal, but cells treated with folate-spm@SSCB[6]VCs did (Fig. 9d), indicating a folate targeting effect for selective cellular uptake into cancer cells. In addition, fluorescent signals were observed in HeLa cells treated with folate-spm@CB[6]VCs, indicating accumulation in the cytosol as dots, unlike the evenly distributed signals inside the nuclei of cells treated with folate-spm@SSCB[6]VCs, indicating a robust membrane structure for amphiphilic CB[6]-based vesicles, and an important role for disulfide linkages in amphiphilic CB[6] for releasing drugs inside cells. Since the surface of SSCB[6]VCs can be decorated with two different functional tags, such as folate-spm and FITC-spm, targeting ligands for cancer cells and image probes can be visualized by confocal laser microscopy, and SSCB[6]VCs can serve as a multifunctional platform for cancer-targeted imaging and drug delivery.

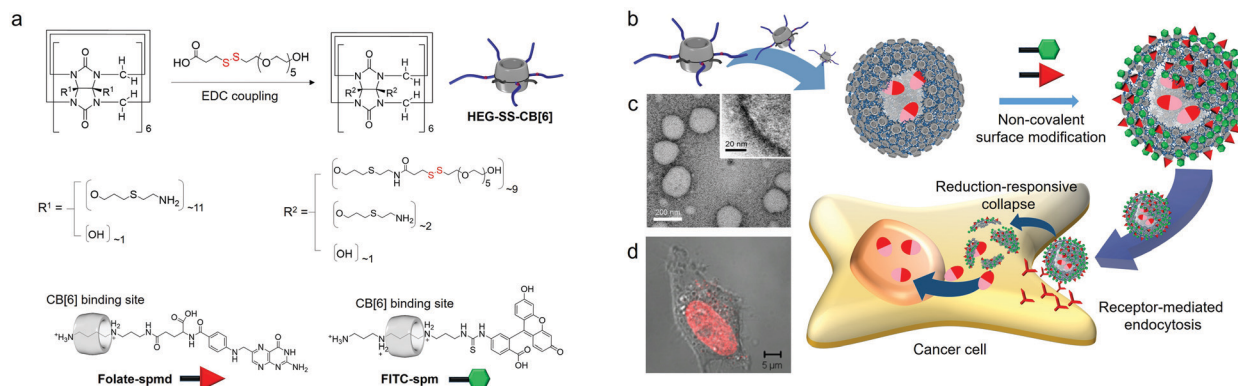


**Fig. 9** Formation of SSCB[6]VCs and their non-covalent surface modification and targeted drug delivery into a HeLa cell. (a) Synthetic scheme of HEG-SS-CB[6]. (b) Chemical structures of FITC-spm and folate-spm. (c) TEM image of SSCB[6]VCs. (d) Confocal laser scanning microscopy image of a HeLa cell treated with DOX-loaded SSCB[6]VCs. TEM and confocal laser scanning microscopy images are reproduced from ref. 34 with permission from Wiley-VCH.



Conjugation of 6-mercaptohexanol with perallyloxyated CB[6] through thiol-ene photoreaction affords hexanol-terminated CB[6] (HOC6-CB[6]; Fig. 10a).<sup>33</sup> Unlike TEG-CB[6] and HEG-SS-CB[6], both of which form vesicles, HOC6-CB[6] self-assembles into micelle-like nanoparticles (CB[6]NPs) with an average diameter of  $\sim 190$  nm (Fig. 10b). Functionalities at the periphery of CB[6] in HOC6-CB[6] are much more hydrophobic than those in TEG-CB[6]; hence HOC6-CB[6] is likely to induce the formation of nanoparticles with a hydrophobic core that can entrap

hydrophobic dyes and anticancer drugs such as Nile Red and paclitaxel, respectively. CB[6]NPs also have a number of CB[6] cavities on their surface; hence CB[6]NPs can be non-covalently yet stably coated with functional tags conjugated to spm (or spmd), forming nanomaterials made of amphiphilic CB[6] derivatives. Efficient release of hydrophobic molecules such as Nile Red inside cancer cells after selective cellular uptake of (FITC-spm and folate-spm)@CB[6]NPs containing Nile Red was visualized by confocal laser scanning microscopy (Fig. 10c), demonstrating the potential of CB[6]NPs for the targeted delivery of hydrophobic drugs for cancer treatment.

Very recently, even a single short arm such as an allyloxy unit was shown to significantly contribute to the amphiphilic nature of CB[7] derivatives. For example, a monoallyloxyated CB[7] derivative (MA-CB[7]) was serendipitously discovered to act as a MA in water, and form a vesicular structure (CB[7]VCs) with an average diameter of 210 nm and a membrane thickness of 3 nm (Fig. 11b(i)).<sup>35</sup> Supramolecular assemblies of MA-CB[7] within membranes are not yet fully understood. Various techniques have been applied to investigate molecular interactions, such as <sup>1</sup>H NMR and high-resolution mass spectrometry, and the results suggest that oligomeric assemblies of MA-CB[7] are formed through intermolecular interactions between allyloxy groups and the portals of different MA-CB[7] molecules, and the resulting assemblies further interact to enclose the membrane and form a vesicle. Since CB[7]VCs entrapping DOX can be internalized into cancer cells such as HeLa cells, as observed by confocal laser scanning microscopy (Fig. 11d), CB[7]VCs can be used as a vehicle for drug delivery. Interestingly, MA-CB[7] is highly susceptible to thiolate molecules such as glutathione (GSH) that convert it into less amphiphilic GSH-conjugated CB[7] (GSH-CB[7]) *via* thiol-ene reactions under light irradiation, resulting in disruption of CB[7]VCs (Fig. 11b(ii) and c). GSH is an endogenous biomolecule present in the cytosol in millimolar concentrations. Thus, CB[7]VCs can be collapsed to release DOX

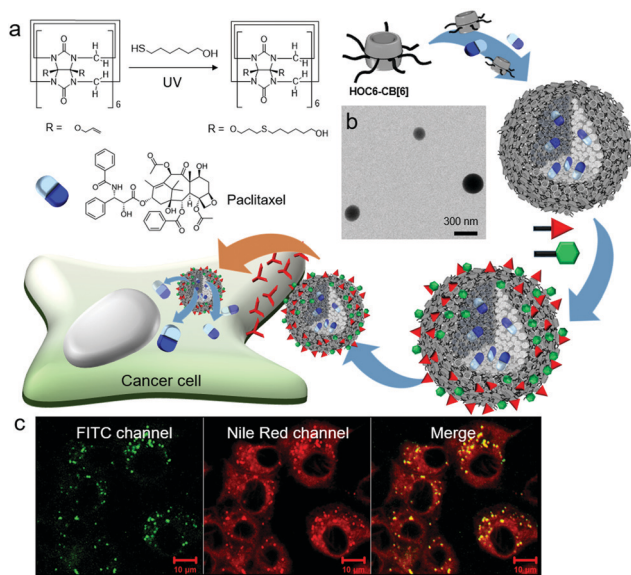


**Fig. 10** Formation of CB[6]NPs, and their non-covalent surface modification and targeted drug delivery into a KB cell. (a) Synthetic scheme of HOC6-CB[6]. (b) TEM image of CB[6]NPs. (c) Confocal laser scanning microscopy image of cells treated with FITC-spm and folate-spm-coated CB[6]NPs containing Nile Red. TEM and confocal laser scanning microscopy images are reproduced from ref. 33 with permission from The Royal Society of Chemistry.

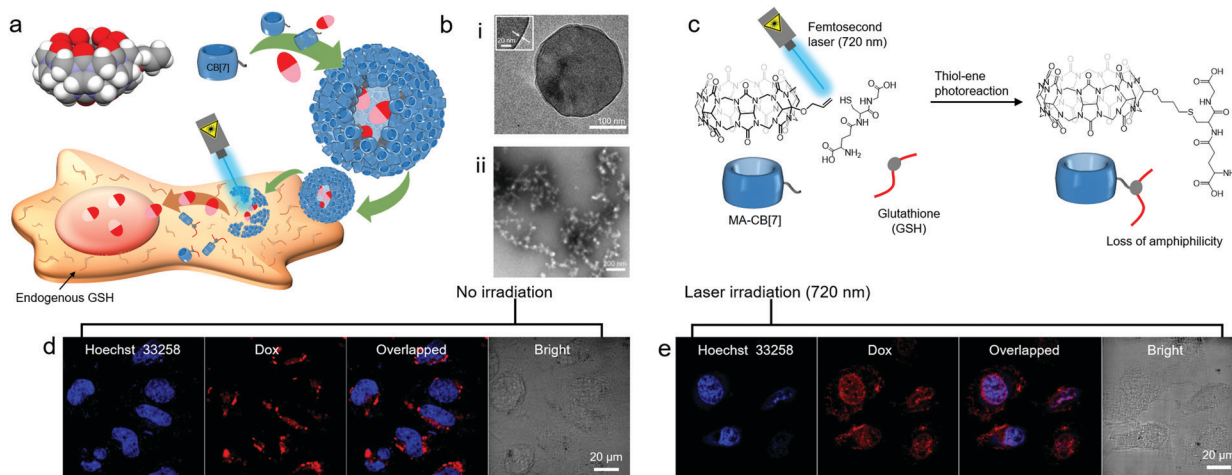


**Fig. 11** (a) Schematic illustration of CB[7]VC formation from MA-CB[7], their non-covalent surface modification and targeted drug delivery into a HeLa cell. (b) TEM images of (i) CB[7]VCs under cryo-conditions and (ii) collapsed CB[7]VCs upon UV irradiation under GSH conditions, (c) light responsive conjugation of GSH to MA-CB[7], confocal laser scanning microscopy images of HeLa cells treated with DOX-loaded CB[7]VCs (d) without and (e) with laser (720 nm) irradiation. TEM and confocal laser scanning microscopy images are reproduced from ref. 35 with permission from Wiley-VCH.

inside cancer cells upon irradiation with light (Fig. 11e). In this study, photoreaction between an allyloxy and a thiol was efficiently induced by the two-photon effect from a femtosecond laser (720 nm), and this proved beneficial for the stimuli-responsive release of drugs since it uses cyto-compatible near-infrared (NIR) light that can penetrate deeper into tissues with less light scattering than UV light. This implies potential applications for CB[7]VCs as on-demand light-responsive drug delivery vehicles that can be used for deep tissue treatment. In addition, like the surface of CB[6]VCs, CB[7]VCs can be coated with functional tags conjugated to a guest of CB[7] such as FITC-conjugated adamantylammonium (FITC-AdA) using stable host-guest chemistry between CB[7] and AdA ( $K_a \sim 10^{13} \text{ M}^{-1}$ ). Like CB[6]VCs, CB[7]VCs are likely to widen the choice of smart functional materials for targeted cancer imaging and controlled release and delivery of drugs.

More recently, Wang and colleagues developed micelle-like nanoparticles formed using an emulsion method with a mixture of perallyloxyated CB[6] and polyvinyl alcohol, by adapting the thiol-ene photoreaction between allyloxy groups on CB[6]-based nanoparticles and endogenous GSH as a means of drug release inside cancer cells.<sup>47</sup> In this study, the hydrophobic drug paclitaxel loaded in the hydrophobic interior of nanoparticles was released selectively inside cancer cells upon irradiation with UVA (present in natural sunlight). Negligible cytotoxicity of the nanomaterial itself and more enhanced cytotoxicity against cancer cells such as melanoma B16 cells than against normal cells illustrates the on-demand release of drugs from nanomaterials in cancer cells upon irradiation by UVA. These results indicate great potential for CB-based self-assembled nanomaterials as a novel light-responsive platform for delivery and controlled release of therapeutics into cancer cells.

## Summary and outlook

As described above, CB[*n*]-based host-guest complexes acting as SAs self-assemble into micelle-like nanoparticles, vesicles, nanosheets, and nanorods. Depending on the combination of host and guest molecules, self-assembled nanomaterials can be responsive to external stimuli such as temperature, pH, acidity, and redox state, thereby transforming their structures into disrupted or other nanostructures. Facile exchange of guests bound to CBs with competitive guests provides another opportunity to tune self-assembled nanostructures and their functions in a simple non-covalent manner. Nanomaterials with these features have potential as smart functional materials for targeted imaging, controlled release and delivery of drugs, and photodynamic therapy. Additionally, conjugation of appropriate functional groups to the periphery of CB[*n*] affords amphiphilic CB[*n*] derivatives as CB[*n*]-based MAs that self-assemble into vesicles or micelle-like nanoparticles. Due to the difficulty in defining hydrophilic and lipophilic units in CB[*n*]-based MAs, understanding their supramolecular packing structures formed within nanomaterials remains challenging. However, CB[6] derivatives with better hydrophilic functional groups on their periphery, such as TEG

and HEG, tend to assemble into vesicles with a robust membrane structure, and other types of amphiphilic CB[6] derivatives with less hydrophilic functional groups such as hexanol assemble into micelle-like nanoparticles with a solid hydrophobic core. By introducing stimuli-responsive chemical linkages such as disulfide bonds into the amphiphile structure, reduction-responsive self-assembled nanomaterials can be developed as smart drug delivery vehicles that release drugs only after being internalized into cells. Surprisingly, MA-CB[7], which has a single short, hydrophobic functionality (allyloxy group) on its periphery, is still amphiphilic and forms CB[7]VCs. High susceptibility of the allyloxy group to endogenous GSH under light irradiation can transform MA-CB[7] into GSH-CB[7], enabling CB[7]VCs to act as on-demand light-responsive drug-releasing nanomaterials inside cancer cells. The large number of CB[6] and CB[7] cavities on the surface of nanomaterials can be exploited by coating the surface with various functional tags conjugated to selected guest molecules (linear polyammonium and adamantyl (or ferrocenemethyl) ammonium for CB[6] and CB[7], respectively) to simultaneously achieve efficient targeting and imaging.

Recently, the host-guest interaction between CB[6] and spmd was revealed to be sufficiently stable to endure the extremely dynamic conditions found in the blood stream, as confirmed by efficient targeted imaging of cancers in mice with intravenously injected CB[6]-based polymer nanocapsules with targeting ligand-spmd and imaging dye-spmd coated on its surface.<sup>48,49</sup> The host-guest interaction between CB[7] and AdA is likely to have similar or even higher stability in animal models since the binding affinity of CB[7]-AdA is two orders of magnitude higher than that of CB[6]-spmd. CB-based materials reported in the literature exhibit negligible toxicity toward cells, even in animals such as *Caenorhabditis elegans* and mice.<sup>48-54</sup>

Current knowledge suggests that CB-based self-assembled nanomaterials can be practically useful for targeted cancer imaging and delivery of drugs. Other types of interesting supramolecular amphiphiles can be afforded by conjugating CB[*n*] to other host molecules (*e.g.*, cyclodextrins, calixarenes, pillararenes, *etc.*). These may self-assemble into various supramolecular structures showing useful functions including sensing, delivery and controlled release for diagnosis and therapy. Furthermore, combining the unique features of host molecule-based supramolecular nanomaterials with those of well-established systems such as polymer-based nano-emulsions and metal organic polyhedron-type molecular cage frameworks as recently demonstrated by Wang<sup>47</sup> and Isaacs,<sup>55,56</sup> respectively, may yield a new class of smart functional nanomaterials for nanotherapeutics and theranostics. To date, most biological studies with CB[*n*]-based nanomaterials have been focused on fundamental *in vitro* experiments and preliminary *in vivo* applications. It is clearly visible that the CB-based biotechnology is progressing towards translational research for effective and practical applications.

## Conflicts of interest

There are no conflicts to declare.

## Acknowledgements

This work was supported by the Institute for Basic Science (IBS) [IBS-R007-D1].

## Notes and references

- 1 A. Sorrenti, O. Illa and R. M. Ortuno, *Chem. Soc. Rev.*, 2013, **42**, 8200–8219.
- 2 S. Fleming and R. V. Ulijn, *Chem. Soc. Rev.*, 2014, **43**, 8150–8177.
- 3 D. Y. Chen and M. Jiang, *Acc. Chem. Res.*, 2005, **38**, 494–502.
- 4 H. Ringsdorf, B. Schlarb and J. Venzmer, *Angew. Chem., Int. Ed. Engl.*, 1988, **27**, 113–158.
- 5 C. Wang, Z. Q. Wang and X. Zhang, *Acc. Chem. Res.*, 2012, **45**, 608–618.
- 6 G. C. Yu, K. C. Jie and F. H. Huang, *Chem. Rev.*, 2015, **115**, 7240–7303.
- 7 X. Zhang and C. Wang, *Chem. Soc. Rev.*, 2011, **40**, 94–101.
- 8 K. Kim, J. Murray, N. Selvapalam, Y. H. Ko and I. Hwang, *Cucurbiturils*, World Scientific (*Europe*), 2018.
- 9 S. J. Barrow, S. Kaser, M. J. Rowland, J. del Barrio and O. A. Scherman, *Chem. Rev.*, 2015, **115**, 12320–12406.
- 10 J. W. Lee, S. Samal, N. Selvapalam, H.-J. Kim and K. Kim, *Acc. Chem. Res.*, 2003, **36**, 621–630.
- 11 Y. H. Ko, E. Kim, I. Hwang and K. Kim, *Chem. Commun.*, 2007, 1305–1315.
- 12 A. E. Kaifer, *Acc. Chem. Res.*, 2014, **47**, 2160–2167.
- 13 L. Isaacs, *Acc. Chem. Res.*, 2014, **47**, 2052–2062.
- 14 E. Masson, X. Ling, R. Joseph, L. Kyeremeh-Mensah and X. Lu, *RSC Adv.*, 2012, **2**, 1213–1247.
- 15 Y. Kim, H. Kim, Y. H. Ko, N. Selvapalam, M. V. Rekharsky, Y. Inoue and K. Kim, *Chem. – Eur. J.*, 2009, **15**, 6143–6151.
- 16 W. S. Jeon, K. Moon, S. H. Park, H. Chun, Y. H. Ko, J. Y. Lee, E. S. Lee, S. Samal, N. Selvapalam, M. V. Rekharsky, V. Sindelar, D. Sobransingh, Y. Inoue, A. E. Kaifer and K. Kim, *J. Am. Chem. Soc.*, 2005, **127**, 12984–12989.
- 17 S. M. Liu, C. Ruscip, P. Mukhopadhyay, S. Chakrabarti, P. Y. Zavalij and L. Isaacs, *J. Am. Chem. Soc.*, 2005, **127**, 15959–15967.
- 18 M. V. Rekharsky, T. Mori, C. Yang, Y. H. Ko, N. Selvapalam, H. Kim, D. Sobransingh, A. E. Kaifer, S. M. Liu, L. Isaacs, W. Chen, S. Moghaddam, M. K. Gilson, K. M. Kim and Y. Inoue, *Proc. Natl. Acad. Sci. U. S. A.*, 2007, **104**, 20737–20742.
- 19 L. P. Cao, M. Sekutor, P. Y. Zavalij, K. Mlinaric-Majerski, R. Glaser and L. Isaacs, *Angew. Chem., Int. Ed.*, 2014, **53**, 988–993.
- 20 D. Shetty, J. K. Khedkar, K. M. Park and K. Kim, *Chem. Soc. Rev.*, 2015, **44**, 8747–8761.
- 21 J. Murray, K. Kim, T. Ogoshi, W. Yao and B. C. Gibb, *Chem. Soc. Rev.*, 2017, **46**, 2479–2496.
- 22 K. I. Assaf and W. M. Nau, *Chem. Soc. Rev.*, 2015, **44**, 394–418.
- 23 M. E. Bush, N. D. Bouley and A. R. Urbach, *J. Am. Chem. Soc.*, 2005, **127**, 14511–14517.
- 24 U. Rauwald, F. Biedermann, S. Deroo, C. V. Robinson and O. A. Scherman, *J. Phys. Chem. B*, 2010, **114**, 8606–8615.
- 25 S. Y. Jon, N. Selvapalam, D. H. Oh, J. K. Kang, S. Y. Kim, Y. J. Jeon, J. W. Lee and K. Kim, *J. Am. Chem. Soc.*, 2003, **125**, 10186–10187.
- 26 D. Lucas, T. Minami, G. Iannuzzi, L. Cao, J. B. Wittenberg, P. Anzenbacher and L. Isaacs, *J. Am. Chem. Soc.*, 2011, **133**, 17966–17976.
- 27 J. B. Wittenberg, M. G. Costales, P. Y. Zavalij and L. Isaacs, *Chem. Commun.*, 2011, **47**, 9420–9422.
- 28 B. Vinciguerra, L. Cao, J. R. Cannon, P. Y. Zavalij, C. Fenselau and L. Isaacs, *J. Am. Chem. Soc.*, 2012, **134**, 13133–13140.
- 29 M. Zhang, L. Cao and L. Isaacs, *Chem. Commun.*, 2014, **50**, 14756–14759.
- 30 N. Zhao, G. O. Lloyd and O. A. Scherman, *Chem. Commun.*, 2012, **48**, 3070–3072.
- 31 K. Kim, N. Selvapalam, Y. H. Ko, K. M. Park, D. Kim and J. Kim, *Chem. Soc. Rev.*, 2007, **36**, 267–279.
- 32 H.-K. Lee, K. M. Park, Y. J. Jeon, D. Kim, D. H. Oh, H. S. Kim, C. K. Park and K. Kim, *J. Am. Chem. Soc.*, 2005, **127**, 5006–5007.
- 33 K. M. Park, K. Suh, H. Jung, D.-W. Lee, Y. Ahn, J. Kim, K. Baek and K. Kim, *Chem. Commun.*, 2009, 71–73.
- 34 K. M. Park, D.-W. Lee, B. Sarkar, H. Jung, J. Kim, Y. H. Ko, K. E. Lee, H. Jeon and K. Kim, *Small*, 2010, **6**, 1430–1441.
- 35 K. M. Park, K. Baek, Y. H. Ko, A. Shrinidhi, J. Murray, W. H. Jang, K. H. Kim, J.-S. Lee, J. Yoo, S. Kim and K. Kim, *Angew. Chem., Int. Ed.*, 2018, **57**, 3132–3136.
- 36 H.-J. Kim, J. Heo, W. S. Jeon, E. Lee, J. Kim, S. Sakamoto, K. Yamaguchi and K. Kim, *Angew. Chem., Int. Ed.*, 2001, **40**, 1526–1529.
- 37 Y. J. Jeon, P. K. Bharadwaj, S. Choi, J. W. Lee and K. Kim, *Angew. Chem., Int. Ed.*, 2002, **41**, 4474–4476.
- 38 D. Z. Jiao, J. Geng, X. J. Loh, D. Das, T. C. Lee and O. A. Scherman, *Angew. Chem., Int. Ed.*, 2012, **51**, 9633–9637.
- 39 X. J. Loh, J. del Barrio, T. C. Lee and O. A. Scherman, *Chem. Commun.*, 2014, **50**, 3033–3035.
- 40 Y. Wang, D. D. Li, H. B. Wang, Y. J. Chen, H. J. Han, Q. Jin and J. Ji, *Chem. Commun.*, 2014, **50**, 9390–9392.
- 41 J. Zhao, C. J. Chen, D. D. Li, X. S. Liu, H. B. Wang, Q. Jin and J. Ji, *Polym. Chem.*, 2014, **5**, 1843–1847.
- 42 D. Wu, Y. Li, J. Yang, J. Shen, J. Zhou, Q. Hu, G. Yu, G. Tang and X. Chen, *ACS Appl. Mater. Interfaces*, 2017, **9**, 44392–44401.
- 43 C. Hu, N. Ma, F. Li, Y. Fang, Y. Liu, L. Zhao, S. Qiao, X. Li, X. Jiang, T. Li, F. Shen, Y. Huang, Q. Luo and J. Liu, *ACS Appl. Mater. Interfaces*, 2018, **10**, 4603–4613.
- 44 V. D. Uzunova, C. Cullinane, K. Brix, W. M. Nau and A. I. Day, *Org. Biomol. Chem.*, 2010, **8**, 2037–2042.
- 45 K. I. Assaf, M. A. Alnajjar and W. M. Nau, *Chem. Commun.*, 2018, **54**, 1734–1737.
- 46 K. Liu, Y. L. Liu, Y. X. Yao, H. X. Yuan, S. Wang, Z. Q. Wang and X. Zhang, *Angew. Chem., Int. Ed.*, 2013, **52**, 8285–8289.
- 47 Q. Cheng, S. Li, C. Sun, L. Yue and R. Wang, *Mater. Chem. Front.*, 2019, **3**, 199–202.
- 48 S. Kim, G. Yun, S. Khan, J. Kim, J. Murray, Y. M. Lee, W. J. Kim, G. Lee, S. Kim, D. Shetty, J. H. Kang, J. Y. Kim, K. M. Park and K. Kim, *Mater. Horiz.*, 2017, **4**, 450–455.
- 49 S. Kim, M. Y. Hur, J. Kim, K. M. Park and K. Kim, *Supramol. Chem.*, 2019, **31**, 289–295.
- 50 K. L. Kim, G. Sung, J. Sim, J. Murray, M. Li, A. Lee, A. Shrinidhi, K. M. Park and K. Kim, *Nat. Commun.*, 2018, **9**, 1712.
- 51 H. Yin and R. B. Wang, *Isr. J. Chem.*, 2018, **58**, 188–198.
- 52 X. J. Zhang, X. Q. Xu, S. K. Li, L. H. Wang, J. X. Zhang and R. B. Wang, *Sci. Rep.*, 2018, **8**, 8819.
- 53 C. Sun, H. Zhang, S. Li, X. Zhang, Q. Cheng, Y. Ding, L.-H. Wang and R. Wang, *ACS Appl. Mater. Interfaces*, 2018, **10**, 25090–25098.
- 54 A. T. Bockus, L. C. Smith, A. G. Grice, O. A. Ali, C. C. Young, W. Mobley, A. Leek, J. L. Roberts, B. Vinciguerra, L. Isaacs and A. R. Urbach, *J. Am. Chem. Soc.*, 2016, **138**, 16549–16552.
- 55 S. K. Samanta, D. Moncelet, V. Briken and L. Isaacs, *J. Am. Chem. Soc.*, 2016, **138**, 14488–14496.
- 56 S. K. Samanta, J. Quigley, B. Vinciguerra, V. Briken and L. Isaacs, *J. Am. Chem. Soc.*, 2017, **139**, 9066–9074.